

## DESIGN AND EXPERIMENT OF SPIRAL-RIBBON BLADE COMBINATION MECHANISM OF STRAW AND MANURE INCLINED MIXING CONVEYOR

### 秸秆粪便斜式混配输送机螺旋-螺带组合机构设计与试验

Tiejun WANG, Peng YIN, Li DU, Rui ZHOU, Yuanjuan GONG, Hongguang CUI<sup>1\*</sup>

Shenyang Agricultural University, College of Engineering, Shenyang / China;

Tel: +8613804060603; E-mail: chg7763@syau.edu.cn

DOI: <https://doi.org/10.35633/inmateh-73-25>

**Keywords:** agricultural machinery; straw; manure; inclined mixing conveyor; spiral blade; ribbon blade

#### ABSTRACT

In order to solve the problem of poor mixing effect of inclined spiral conveyor, this paper designed an inclined spiral and ribbon blade combination conveying device. The mechanics and kinematics analysis of the movement process of the material unit in each mechanism was carried out, on which key devices and components were designed based. Effects of the speed of main shaft ( $X_1$ ), the full coefficient ( $X_2$ ) and the angle of inclination ( $X_3$ ) on the mixing uniformity ( $Y_1$ ) and the residual rate of material ( $Y_2$ ) were explored. Three-dimensional quadratic regression orthogonal rotation central combination experiment method combined with response surface method was used to conduct experiments and explore the interaction effects of influence factors on indicators. A regression model of influence factors and evaluation indicators was established through the analysis of variance. The significant factors affecting  $Y_1$  were ordered of  $X_3$ ,  $X_2$ ,  $X_1$ , and the significant factors affecting  $Y_2$  were ordered of  $X_2$ ,  $X_1$ , and  $X_3$ . In the interaction of factors,  $X_1X_2$  had a significant impact on  $Y_1$  and  $Y_2$ ;  $X_1X_3$  had an extremely significant impact on  $Y_1$ ;  $X_2X_3$  had an extremely significant effect on  $Y_1$  and a significant impact on  $Y_2$ . The optimal structure and working parameters combination were determined to be 50 rpm for the speed of main shaft, 60% for the full coefficient, and 19° for the angle of inclination, while the verification experiments demonstrated that the mixing uniformity and residual rate of material corresponding to the verification test were 90.37% and 5.31%, respectively. The inclined device with combined spiral and ribbon blade developed in this study meets the design requirements for the misprocess of the fertilizer utilization of agricultural organic wastes.

#### 摘要

为解决倾斜螺旋叶片输送机输送秸秆与畜禽粪便混合效果不佳的问题，设计了一种适用于作物秸秆与畜禽粪便混合用于肥料生产的螺旋叶片与螺带叶片组成的斜式混合输送装置，并对其进行了设计和性能试验。结合物料单元体在关键机构中的动力学与运动学分析，确定机构主要结构及工作参数。采用三元二次回归正交旋转中心组合试验方法，以主轴转速、充满系数和倾斜角度为试验因素，以混合均匀度和物料残留率为评价指标，实施试验并对其结果进行分析，建立影响因素与评价指标回归模型。结果表明：影响混合均匀度的主次因素是倾斜角度、充满系数、主轴转速，影响物料残留率的主次因素是充满系数、主轴转速、倾斜角度；确定最优参数组合为：主轴转速 50 r/min、充满系数 60%、倾斜角度 19°，在此条件下混合均匀度和物料残留率分别达到 90.37%、5.31%，试验验证结果表明，所设计机构满足技术要求。

#### INTRODUCTION

Crop straw and livestock manure are important fertilizer source materials for organic fertilizers (Dong et al., 2019; Chen et al., 2020). Their mixing and transportation links are important factors affecting the quality and efficiency of fertilizer production (Li et al., 2012). The integrated treatment of mixing and transportation can ensure the production quality and improve the production efficiency of fertilizer production at the same time (Ştefan et al., 2019&2021). The research and development of small-scale mixed transportation collaborative operation devices can provide technical support for improving the utilization rate of agricultural waste in local fertilizer (Zhang et al., 2020).

Researchers at domestic and abroad explored the mixing and conveying mechanism of agricultural waste. Such as straw and cow manure from the perspective of material flow characteristics and mechanical working parameters through experimental optimization and simulation (Chupshev et al., 2019; Savinyh et al., 2020; Sakai et al., 2015). The solid mixing test to the twin spiral ribbon mixer can be used to simulate the mixing uniformity and the torque of the mixing shaft with DEM of packing height and blade speed (Simons et al., 2016).

EDEM software was used to simulate and analyse the flow characteristics of corn stalk powder under the current working conditions of the spiral feeder. LIGGGHTS (LAMMPS improved for general granular and granular heat transfer simulations) software was used to solve the discrete element model to study the effects of rotational speed, filling rate, particle number ratio and loading mode on the mixing quality of dispersed particles in the horizontal blade mixer. It is found that the particle number ratio has the greatest effect on the mixing performance, and diffusion mixing has more advantages than convection mixing (Mohammadreza *et al.*, 2020).

The installation experiment stand of horizontal screw conveying device was built, and a spiral-pneumatic coupling conveying device was designed, which provided a feasible device structure for the study of screw conveying and kneading corn stalk (Wulantuya *et al.*, 2016 & 2019). The scholars quantitatively analysed the motion characteristics of straw particles by means of the discrete element method, high-speed tracer particle photography and comparison of test images, which provided a better analysis method for obtaining appropriate discrete element parameters and motion rules of material characteristics (Ştefan *et al.*, 2018; Feng *et al.*, 2017; Zhou *et al.*, 2015). The scholars researched on ration mixers with different mixing components through high-speed photography technology, that provided an effective way to analyse the mixing process and type distribution of materials, the relationship between work and structural parameters and special mixing phenomena (Wang *et al.*, 2017; Li *et al.*, 2017; Wang *et al.*, 2020; Yu *et al.*, 2015).

Aiming at the problems such as unsatisfactory mixing effect, not applicable for material mixing, and no function of conveying material in horizontal spiral ribbon mixing, this paper designs a spiral-ribbon inclined mixing conveyor device for crop straw and manure production. Based on the dynamic and kinematic analysis and test of the material unit in each mechanism of the device, the influence of the key structure, working parameters and their interaction on the production capacity and working effect of the device is analysed and verified. The optimal structure and working parameters are proposed to realize the integrated treatment of the mixed transportation of crop straw, manure and sewage in the process of fertilizer production.

## MATERIALS AND METHODS

### Machine structure and working principle

The structure of the straw manure inclined mixing conveyor is shown in Fig.1, which is mainly composed of spiral blade, spiral ribbon blade, mechanical housing, support, spindle, frame, motor. The spindle can adjust the horizontal angle between the spindle and the ground under the action of the electric push rod support. From bottom to top, spiral blade with equal pitch, spiral ribbon blade with equal pitch, and spiral blade with variable pitch are arranged along the spindle in order to realize the mixing and transportation of straw manure under inclined conditions according to the principle of convection and shear mixing.

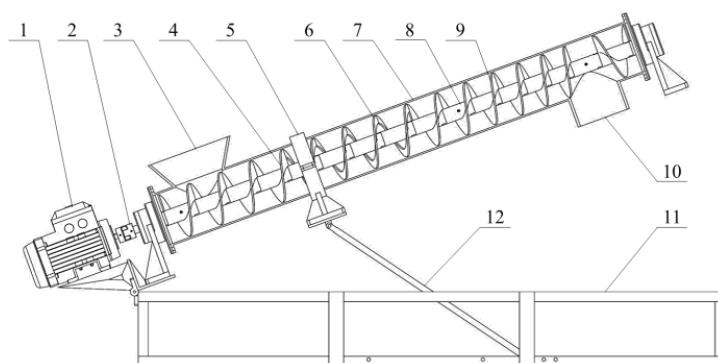


**Fig. 1 - Machine structure diagram**

1- Speed regulating motor; 2- Coupling; 3- Feeding port; 4- Equal pitch spiral mechanism; 5- Support; 6- Equal pitch spiral ribbon mechanism; 7- Mechanical housing; 8- Spindle; 9- Variable pitch spiral mechanism; 10- Discharge port; 11- Frame; 12- Angle adjustment bracket

When the machine works, the crushed straw, livestock and poultry manure enter through the feeding port 3 and are transported to the discharge port 10 in the spiral direction. Materials are pre-mixed in the vertical direction of each spiral section of the equal pitch spiral mechanism 4, and secondary mixing is carried out in the horizontal and vertical directions of the hollow structure of the spiral ribbon blade of the equal pitch spiral mechanism 6 in each spiral section. That is, the unmixed materials have different movements due to the difference in forces in every direction, resulting in the coexistence of multiple mixing forms such as convection and shear. Therefore, the variable pitch spiral mechanism 9 is recompressed along the decreasing pitch direction and finally discharged downward through the discharge port 10, at the upper end of the device.

**Analysis and design of key components**

The spiral-ribbon combined mechanism is the key component of the inclined mixing conveyor, which directly affects the performance of the mixing conveyor. The horizontal angle of the spindle is the main parameter reflecting the mixing force of the spiral ribbon mechanism on the straw manure material, and the spiral lift angle is the main parameter reflecting the spiral mechanism on the straw manure material conveying force. Refer to the main parameter relation of spiral conveying mechanism:

$$Q = 47 D^2 \Psi S n \gamma C \tag{1}$$

where:  $Q$  is the productivity, kg/h;  $D$  is the outer diameter of the helix, m;  $\Psi$  is the full coefficient;  $S$  is the pitch, m;  $n$  is the speed of main shaft, r/min;  $\gamma$  is the bulk weight of the material, kg/m<sup>3</sup>;  $C$  is the inclination correction factor, the corresponding value is taken according to the inclination angle.

In this paper, the relevant parameters are determined based on the operation conditions and requirements such as the fertilizer source material ratio, the geometric length range of straw silk, and the unit power productivity of the previous straw kneading process determined by the research group's previous research results (Wang et al., 2021a & 2021b). The design machine productivity  $Q=800$  kg/h, material bulk weight  $\gamma=200$  kg/m<sup>3</sup>, equal pitch spiral (spiral ribbon) mechanism  $D=2R_1=2R_2=0.30$  m, the width of spiral ribbon mechanism  $d=0.1D=0.03$  m, the spiral pitch of equal pitch spiral (spiral ribbon) mechanism  $S_1=S_2=0.10$  m. The mechanism designed in this paper operates in the inclined state. When the full coefficient takes down the limit value 0.4 and the inclination angle takes up the upper limit value, that is,  $C_{min}=0.4$ ,  $n_{max}=59.10$  rad/min.

While determining the design parameters, it is necessary to further determine the main factors affecting the working performance of the spiral-ribbon combined device through the force and movement analysis of the material (Ştefan et al., 2017). Straw and manure materials are regarded as material unit with a mass of  $m$  in the analysis, and it is assumed that the friction factors between all parts at any position in the device are  $f$ , and the friction angles between materials and components are  $\varphi$ . The quality of materials in the space of the equal pitch spiral and spiral ribbon mechanism in the device is the same. According to the helical lift angle and other conditions, the effect of the force in the spiral blade plane is transformed into the projected amount of the force in the vertical and horizontal xOy planes formed along the main axis.

**Equal pitch spiral mechanism**

The simplified force analysis of the material unit in the equal pitch spiral mechanism is shown in Fig. 2.

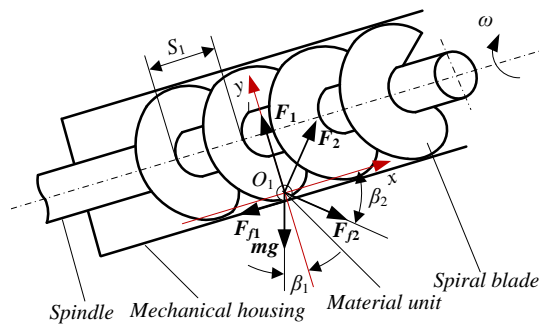


**Fig. 2 - Force analysis diagram of material unit in oblique spiral mechanism with equal pitch**

Note:  $F_1$  is the supporting force of the mechanical housing on the material unit, N;  $F_2$  is the positive pressure of the spiral blade with equal pitch on the material unit in xO<sub>1</sub>y plane, N;  $F_{f1}$  is the friction force between the mechanical housing and the material unit, N;  $F_{f2}$  is the friction force between the equal pitch spiral blade and the material unit in the xO<sub>1</sub>y plane, N;  $\omega$  is the angular speed of the spindle rotation, rad/s;  $\beta_1$  is the horizontal inclination angle of the main shaft, °;  $\beta_2$  is the lift angle of the equal pitch spiral blade, °.

The three-dimensional space motion equation of the material unit is established from Fig. 2. The contact position between the material element and the surface of the spiral blade and the surface of the casing is determined by the radius  $R$  of the spiral blade and the displacement angle  $\beta_0$  (Hewko et al., 2015). In the hypothetical case, the coordinates of the material unit are determined by Eq. (2):

$$\begin{cases} x_A = (R_1 - K) \cos \beta_0 + K \cos^2 \beta_0 \\ y_A = R_1 \sin \beta_0 \\ z_A = \frac{S_1(\omega t_1 - \beta_0)}{2\pi} \end{cases} \tag{2}$$

where:

$x_A$  is the  $x$  coordinate of the material unit in the process of the equal pitch spiral mechanism movement, m;  $y_A$  is the  $y$  coordinate of the material unit during the motion of the constant pitch spiral mechanism, m;  $z_A$  is the  $z$  coordinate of the material unit during the motion of the constant pitch spiral mechanism, m;  $R_1$  is the spiral radius of the equal pitch spiral mechanism, m;  $\beta_0$  is the displacement angle of the material unit during the motion of the equal pitch spiral mechanism, rad;  $t_1$  is the movement time of the material unit, s;  $K$  is the material coefficient;  $S_1$  is the pitch, mm.

It can be seen from Eq. (2) that when the spiral radius  $R$  and pitch  $S$  are fixed, the displacement and acceleration of the material during movement are related to the speed of main shaft  $n$  and the inclination angle  $\beta_1$ . The appropriate range should be determined to meet the design requirements.

**Spiral ribbon mechanism with equal pitch**

The simplified force and motion analysis of the material unit in the spiral ribbon mechanism are shown in Fig. 3. As can be seen from Fig. 3a, the conditions to ensure the movement of materials along the spiral direction are:

$$\begin{cases} \sum F_{x2} = F_4 \sin \beta_3 + F_{f4} \cos \beta_3 - F_{f3} - F_{f5} - mg \sin \beta_1 \geq 0 \\ \sum F_{y2} = F_3 + F_4 \cos \beta_3 - F_{f4} \sin \beta_3 - F_5 - mg \cos \beta_1 \geq 0 \end{cases} \quad (3)$$

where:  $F_{x2}$  is the resultant force of the material unit in the  $x$  direction during the movement of the constant pitch spiral ribbon mechanism, N;  $F_{y2}$  is the resultant force of the material unit in  $y$  direction during the movement of the constant pitch ribbon mechanism, N.

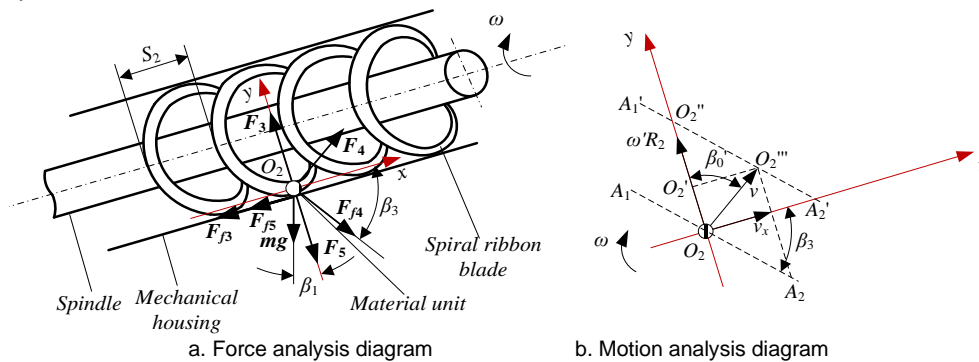


**Fig. 3 - Force and motion analysis diagram of material unit in oblique spiral ribbon mechanism with equal pitch**

Note:  $F_3$  is the supporting force of the mechanical housing on the material unit in oblique spiral ribbon mechanism with equal pitch, N;  $F_4$  is the positive pressure of the spiral ribbon blade on the material unit in  $xO_2y$  plane, N;  $F_5$  is the pressure of the upper material on the material unit during the movement of the equal pitch spiral ribbon mechanism, N;  $F_{f3}$  is the friction force between the mechanical housing and the material unit in oblique spiral ribbon mechanism with equal pitch, N;  $F_{f4}$  is the friction force between the spiral ribbon blade and the material unit in the  $xO_2y$  plane, N;  $F_{f5}$  is the friction force between the materials in oblique spiral ribbon mechanism with equal pitch, N;  $\beta_3$  is the lift angle of the equal pitch spiral ribbon blade, °.

According to Coulomb's formula:

$$\tan \beta_1 \leq \frac{F_4 (\sin \beta_3 + \tan \varphi \cos \beta_3) - (F_3 + F_5) \tan \varphi}{F_4 (\cos \beta_3 - \tan \varphi \sin \beta_3) + F_3 - F_5} \quad (4)$$

The motion analysis of the material unit in the constant pitch spiral ribbon mechanism is shown in Fig. 3b. After  $t_2$  time of movement, the material unit moves in a circle with the angular speed  $\omega'$  less than the rotation of the main shaft, resulting in displacement  $l_{O_2O_2}$ . Relative movement with the spiral ribbon blade at the same time results in displacement  $l_{O_2O_2''}$ .

$$v^2 = v_x^2 + v_y^2 = v_x^2 + (\omega R_2 - \tan \beta_3 v_x)^2 \quad (5)$$

$$\tan \beta_0' = \frac{l_{O_2'O_2''}}{l_{O_2'O_2}} = \frac{l_{O_2'O_2''}}{l_{O_2'O_2} - \tan \beta_3 l_{O_2'O_2}} = \frac{v_x}{\omega R_2 - \tan \beta_3 v_x} \quad (6)$$

where:  $v$  is the speed of the material unit in the constant pitch spiral ribbon mechanism, m/s;  $v_x$  is the axial component velocity of the material unit during the movement of the constant pitch ribbon mechanism, m/s;  $v_y$  is the radial component velocity of the material unit during the movement of the constant pitch ribbon mechanism, m/s;  $R_2$  is the spiral radius of the constant pitch ribbon mechanism, m;  $\beta_0'$  is the displacement angle of the material unit during the movement of the constant pitch spiral ribbon mechanism, rad.

According to the theorem of kinetic energy, the force between matter and material  $F_5$ , can be expressed as:

$$F_5 = m \frac{v^2}{R_2} \tag{7}$$

The instantaneous inter body force of the material unit can be obtained by connecting the vertical Eqs. 3-7:

$$F_5 = \frac{m\omega^2 R_2}{1 + \tan \beta_0 \tan \beta_3} \left( \frac{1}{1 + \tan \beta_0 \tan \beta_3} + \tan^2 \beta_0' \right) \tag{8}$$

When the force between the material unit overcomes its own gravity ( $F_5 \geq mg$ ), and achieves the best mixing effect along the negative direction of the  $x$  axis ( $\beta_0' = -90^\circ$ ), then the speed of main shaft  $n_{\min} = 25 \text{ rad/min}$ .

**Spiral mechanism with unequal pitch**

The simplified force analysis of the material unit in the variable pitch spiral mechanism is shown in Fig. 4. During the movement of the variable pitch spiral mechanism, the material unit is subjected to the following forces: Its own gravity  $mg$ , the thrust  $F_6$  and friction force  $F_{f6}$  of the rear material, the positive pressure  $F_7$  and friction force  $F_{f7}$  of the spiral blade behind the forward direction, the positive pressure  $F_8$  and friction force  $F_{f8}$  of the spiral blade in the forward direction, the resistance  $F_{f8}$  and friction force  $F_{f9}$  of the front material, the pressure  $F_{10}$  and friction force  $F_{f10}$  of the mechanical housing.

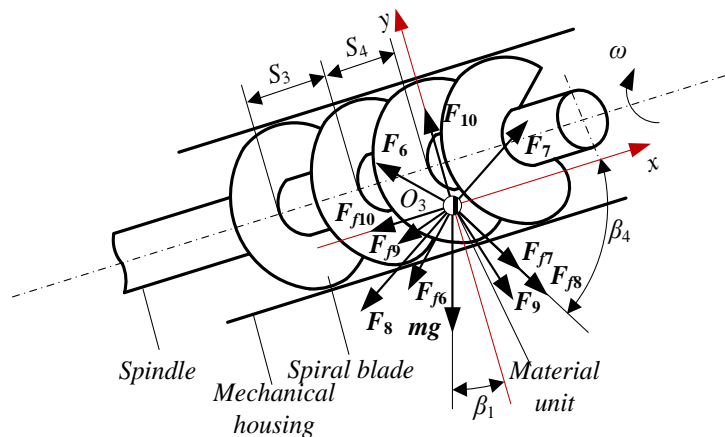


Fig. 4 - Force analysis diagram of material unit in oblique spiral mechanism with unequal pitch

The variable pitch spiral mechanism belongs to the quantitative variable pitch spiral structure, in which the movement law of each monomer material in the bin is not the same, and there are irregular changes due to the change of spiral moment. To ignore the difference between monomer material and the interaction force between materials, the calculation formula of the quantitative variable pitch spiral structure flowmeter is adopted (Xu et al., 2021):

$$Q = \frac{E \cdot 60 \gamma \psi n L}{10^9} = \frac{47 D^2 \gamma \psi n \sum_{i=3}^t S_i^2}{t S_3 + (t-1) S_4 + (t-2) S_5 + \dots + S_t} \tag{9}$$

where:

$E$  is the blanking volume per turn per unit length,  $\text{m}^3$ ;  $L$  is the length of the spiral body,  $\text{mm}$ ;  $t$  is the serial number of the spiral segment.

The length of the variable pitch spiral mechanism is designed  $L = 400 \text{ mm}$ , and five spiral segments are designed, which are  $S_3$  to  $S_7$ . According to Eq. (9), when the actual blade diameter, filling rate, density and rotational speed are fixed, the influence of the variable pitch of the feed section on the flow rate is mainly considered. Concerning Xu et al. (2021), the design values of the spiral pitch in the variable pitch mechanism are  $S_3 = 0.10 \text{ m}$ ,  $S_4 = 0.09 \text{ m}$ ,  $S_5 = 0.08 \text{ m}$ ,  $S_6 = 0.07 \text{ m}$  and  $S_7 = 0.06 \text{ m}$ , respectively.

To sum up, to further clarify the influence of the speed of main shaft, full coefficient and inclination angle on the mixing effect and conveying capacity of the machine, this paper carries out experimental analysis and optimization.

## Experiment design

### Experiment condition

The experiment was carried out at the Northeast Horticultural Engineering Scientific Observation Station of the Ministry of Agriculture and Rural Affairs. The experimental straw was harvested and air-dried corn straw (variety: *Wanying 178*) from Beishan Scientific Research Base of Shenyang Agricultural University. The manure for the experiment was taken from fresh manure of surrounding farmers. The experiment fertilizer source material ratio (corn straw dry matter mass to fertilizer mass ratio) was 23%. The geometric length of straw silk was 10 to 50 mm (Wang *et al.*, 2017a). The average moisture content of straw and cow manure was 15.36% and 65.12%, respectively.

Experiment equipment included electronic analysis balance (Germany Sartoris QUINTIX224-1CN), digital display electric constant temperature drying oven (Shanghai Sunshine Experimental Instrument Co., LTD. 101-0A), DC regulated power supply (Yuride UTP1306S), variable-speed motor (Pfield 10RK60RGN-CF), incline meter (homemade), electronic scale.

### Experiment factors and indexes

Three-dimensional quadratic regression orthogonal rotation central combination experiment method, combined with response surface method, was used to conduct experiments and explore the interaction effects of influence factors on indicators. Effects of the speed of main shaft ( $X_1$ ), the full coefficient ( $X_2$ ) and the angle of inclination ( $X_3$ ) on the mixing uniformity ( $Y_1$ ) and the residual rate of material ( $Y_2$ ) were explored.

According to the relevant research on the mixing characteristics of materials and the comparative analysis of the theory and test of the detection method of mixing uniformity (Wulatuya *et al.*, 2016; Wang *et al.*, 2013), the physical method was adopted in this experiment, the soybean (the variety was Dongdou NO.1) was used as the tracer to detect the mixing uniformity. According to the total mass of the feeding material in each experiment level, the corresponding quality of soybeans were put in equal proportion (from the thousand grain weight of soybeans to the corresponding quality of the feeding material), so that the quality of soybeans in the unit mass of the feeding material was equal, which was regarded as the quantity of soybeans contained in the unit mass of the feeding material was equal. During the experiment, the samples were taken 10 times at the outlet at the same time interval, about 250 g each time. The parameter value of the tracer quantity under the experiment level was calculated with the corresponding value  $n_i$  of the tracer quantity measured at each time, and the mixing uniformity  $Y_1$  (%) was calculated according to Eq. (10). The material quality was weighed before and after each level experiment, and the material residue rate  $Y_2$  (%) was calculated according to Eq. (11).

The experiment process and samples were shown in Fig. 5. According to the analysis of the aforementioned documents and the mixing process, the value range of each factor and the experiment factor levels were shown in Table 1.

$$Y_1 = (1 - S/\bar{n}) \times 100\% \quad (10)$$

$$Y_2 = (T_1 - T_2)/T_1 \times 100\% \quad (11)$$

where:

$S$  is the standard deviation of the number of tracers;  $\bar{n}$  is the average value of the number of tracers;  $T_1$  is the mass of the feed-in material, kg;  $T_2$  is the mass of discharged material, kg.



Fig. 5 - Experimental apparatus (left) and collected sample (right)

Table 1

Factors and levels of combination experiment

Levels	Factors		
	Speed of main shaft	Full coefficient	Inclination angle
	[r·min <sup>-1</sup> ]	[%]	[°]
	X <sub>1</sub>	X <sub>2</sub>	X <sub>3</sub>
1.682	60.00	80.00	35.00
1	52.90 (53.00)	71.89 (72.00)	29.93 (30.00)
0	42.50	60.00	22.50
-1	32.10 (32.00)	48.11 (48.00)	15.07 (15.00)
-1.682	25.00	40.00	10.00
Δj	10.40 (10.50)	11.89 (12.00)	7.43 (7.50)

Note: The parameters in parentheses were the parameters taken in the experiment. Adjusted the calculation results according to the feasibility of actual operation, and taken the values in parentheses.

**RESULTS**

A total of 23 groups of experiment were considered, and each group was repeated three times. The results were taken as the average value. The experiment scheme design and result analysis were shown in Table 2, where X<sub>1</sub>, X<sub>2</sub>, and X<sub>3</sub> are factor coded values specified in Table 1. Using Design-Expert software, multiple regression analysis was carried out by mixing uniformity Y<sub>1</sub> and material residue rate Y<sub>2</sub> as response indexes, and speed of main shaft, full coefficient, and inclination angle as influencing factors to obtain the regression model.

Table 2

Experimental plan and results

No.	Speed of main shaft	Full coefficient	Inclination angle	Y <sub>1</sub>	Y <sub>2</sub>
	[r·min <sup>-1</sup> ]	[%]	[°]	[%]	[%]
1	1	1	1	81.12	6.84
2	1	1	-1	93.73	6.90
3	1	-1	1	80.14	3.32
4	1	-1	-1	84.41	4.87
5	-1	1	1	80.88	8.18
6	-1	1	-1	87.41	7.89
7	-1	-1	1	80.58	6.15
8	-1	-1	-1	82.24	6.88
9	1.682	0	0	84.29	5.41
10	-1.682	0	0	80.13	7.85
11	0	1.682	0	85.49	7.95
12	0	-1.682	0	80.68	3.80
13	0	0	1.682	80.46	5.81
14	0	0	-1.682	90.89	7.88
15	0	0	0	88.22	5.56
16	0	0	0	87.72	5.73
17	0	0	0	87.17	4.85
18	0	0	0	88.79	5.04
19	0	0	0	88.26	5.19
20	0	0	0	87.24	4.80
21	0	0	0	87.40	5.31
22	0	0	0	86.67	5.39
23	0	0	0	88.77	5.44

**Experiment results variance analysis**

It can be seen from Table 3, the effects of the speed of main shaft (X<sub>1</sub>), full coefficient (X<sub>2</sub>), and inclination angle (X<sub>3</sub>) on mixing uniformity and material residue rate were very significant (P<0.01). The secondary terms of speed of main shaft and inclination angle had great significant effects on mixing uniformity and material residue rate (P<0.01). The quadratic terms of the full coefficient had a great significant influence on the mixing uniformity (P<0.01) and have a significant influence on the material residue rate (P<0.05).

Table 3

Data significance experiment and analysis of variance

Source of variation	The mixing uniformity $Y_1$				The residual rate of material $Y_2$			
	SS	DF	F value	P value	SS	DF	F value	P value
Model	328.72	9	62.42	<0.0001**	39.35	9	37.95	<0.0001**
$x_1$	17.07	1	29.18	0.0001*	9.3	1	80.74	<0.0001**
$x_2$	41.72	1	71.29	<0.0001**	17.79	1	154.41	<0.0001**
$x_3$	132.97	1	227.24	<0.0001**	2.23	1	19.38	0.0007**
$x_1x_2$	2.9	1	4.96	0.0442*	0.7859	1	6.82	0.0215*
$x_1x_3$	9.44	1	16.13	0.0015**	0.1685	1	1.46	0.2481
$x_2x_3$	21.79	1	37.24	<0.0001**	0.7839	1	6.8	0.0217*
$x_1x_1$	56.97	1	97.36	<0.0001**	3.31	1	28.76	0.0001**
$x_2x_2$	39.9	1	68.18	<0.0001**	0.5668	1	4.92	0.0450*
$x_3x_3$	7.11	1	12.14	0.0040**	4.5	1	39.04	<0.0001**
Lack of Fit	3.15	5	1.13	0.417	0.7023	5	1.41	0.3156

Among the interaction factors, the interaction of the speed of main shaft and full coefficient ( $X_1X_2$ ) had significant effects on mixing uniformity and material residue rate ( $P<0.05$ ). The interaction of the speed of main shaft and inclination angle ( $X_1X_3$ ) had a great significant effect on the mixing uniformity ( $P<0.01$ ). The interaction between the full coefficient and the inclination angle ( $X_2X_3$ ) had a great significant effect on the mixing uniformity ( $P<0.01$ ) and a significant effect on the material residue rate ( $P<0.05$ ). The coefficient of determination is  $R_1^2=0.98$ ,  $R_2^2=0.96$ . The significant level  $F_R$  of the regression equation, the  $F_{L_f}$  value and  $P$  value of the mismatch experiment were greater than 0.05, indicating that the relationship between the regression equation were statistically significant. At the significant level of  $P=0.05$ , non-significant items were eliminated and the regression model of each factor and index  $Y$  was simplified as follows:

$$\hat{Y}_1 = 87.80 + 1.12X_1 + 1.75X_2 - 3.12X_3 + 0.60X_1X_2 - 1.09X_1X_3 - 1.65X_2X_3 - 1.89X_1^2 - 1.58X_2^2 - 0.67X_3^2 \quad (12)$$

$$\hat{Y}_2 = 5.26 - 0.83X_1 + 1.14X_2 - 0.40X_3 + 0.31X_1X_2 + 0.31X_2X_3 + 0.47X_1^2 + 0.19X_2^2 + 0.53X_3^2 \quad (13)$$

**Analysis of influencing factors**

The calculation results of the response surface of each experiment factor and its interaction on the experiment index were shown in Fig. 6. It can be seen from the figure that the primary and secondary order of the influence of each experiment factor on the mixing uniformity was inclination angle>full coefficient>speed of main shaft; and the primary and secondary order of the influence of each experiment factor on the material residual rate was full coefficient>speed of main shaft>inclination angle.

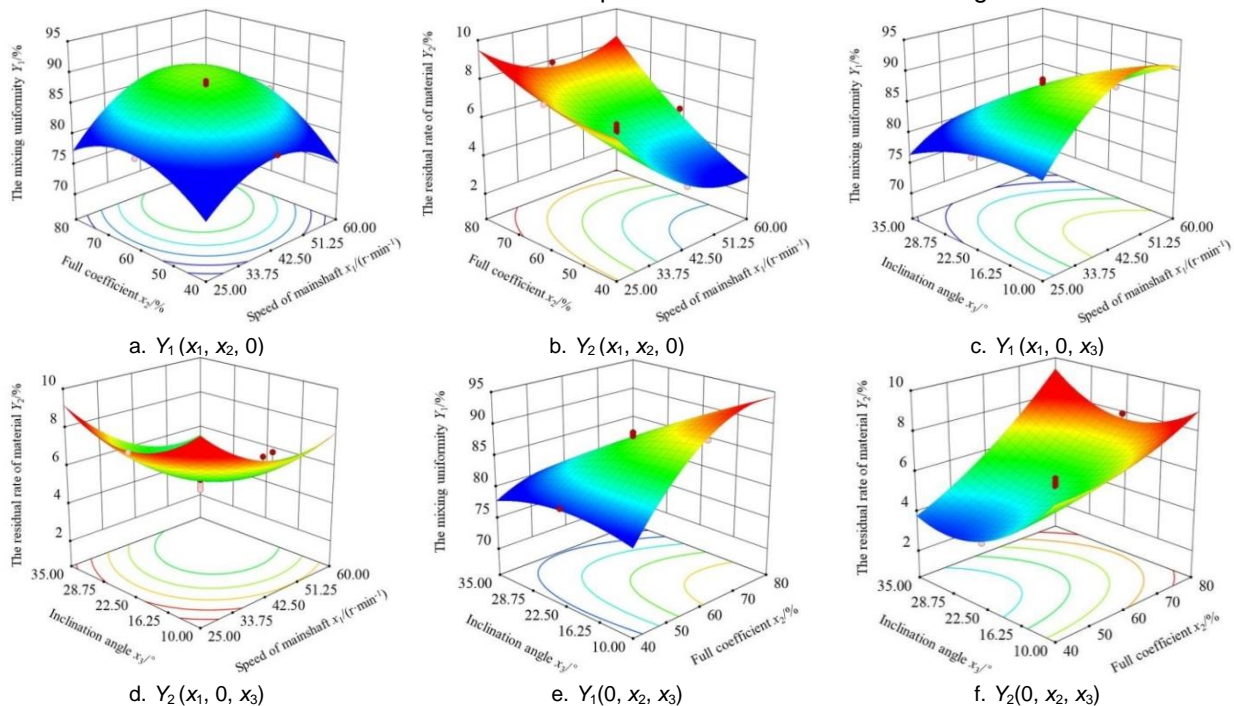


Fig. 6 - Response surface analysis of the factors' interaction effect on the index



Fig. 6a and 6b showed the response surface diagram of the influence of the speed of main shaft and full coefficient interaction ( $X_1X_2$ ) on  $Y_1$  and  $Y_2$  when the inclination angle ( $X_3$ ) was zero level value ( $22.50^\circ$ ). The analysis showed that when  $X_1$  and  $X_2$  gradually increase within the experiment range,  $Y_1$  first increases and then decreases, and  $Y_2$  gradually increases. When  $x_2$  was constant and  $x_1$  increases gradually within the experiment range,  $Y_1$  also increases first and then decreases, and  $Y_2$  gradually decreases. At the same time,  $x_2$  determines the total amount of the materials in the device per unit of time. When  $x_2$  value was low, there was less material, the active diffusion movement ability between materials was weak, the shear effect of mixing parts on materials was reduced, the mixing effect was unsatisfactory, and the materials were less attached to the shell and the mixing mechanism. When the  $x_2$  value was high, there were more materials, and the diffusion effect between materials was limited by the movement space. Meanwhile, under the same speed (under the power input) the driving force of the stirring parts was more dispersed, which affected the convective mixing process and reduces the mixing effect, and more materials were attached to the housing and stirring parts. When  $x_2$  was constant, increasing  $x_1$  appropriately to transport power input could improve the mixing effect, but when  $x_1$  was too large, the input power was larger, driving the material movement speed up, and the material residue was less, but different bulk weight materials were easy to form different mixing material areas in the housing, resulting in uncoordinated convection and diffusion movement conditions in the horizontal and vertical directions of the material, thus reducing the mixing effect.

Fig. 6c and 6d showed the response surface diagram of the influence of the interaction between the speed of main shaft and inclination angle ( $X_1X_3$ ) on  $Y_1$  and  $Y_2$  when the full coefficient ( $X_2$ ) was zero horizontal value (60%). According to the analysis, when  $X_1$  was constant and in the lower level of the experiment range, when  $X_3$  gradually increased in the experiment range,  $Y_1$  first increases and then decreases, and  $Y_2$  first decreases and then increases with the increase of  $X_3$ . When  $X_1$  was constant and in the higher level of the experiment range,  $X_3$  gradually increases in the experiment range,  $Y_1$  and  $Y_2$  gradually decrease. When  $X_3$  and  $X_1$  gradually increase within the experiment range,  $Y_1$  first increases and then slightly decreases, and  $Y_2$  gradually decreases. This was because when  $X_2$  was certain, that is, the total amount of materials in the device in unit time was the same; the same  $X_3$  meant the same material was subject to the same external force in unit time. Increasing  $X_1$  increased the disorderly motion speed of the material, thereby improving the mixing effect, and reducing the time of material attachment to the housing and accumulation on the mixing parts, thus increasing the discharge and reducing the material residual rate.

Fig. 6e and 6f were the response surface diagrams of the influence of the full coefficient and inclination angle interaction ( $X_2X_3$ ) on  $Y_1$  and  $Y_2$  when the speed of main shaft ( $X_1$ ) was zero horizontal value (42.5 r/min). It could be seen from the analysis that if  $X_2$  was a fixed value, when  $X_3$  gradually increased in the lower level of the experiment range,  $Y_1$  had insignificant change, and  $Y_2$  first decreases and then slightly increases. If  $X_2$  was a fixed value, when  $X_3$  gradually increased in the higher level of the experiment range,  $Y_1$  gradually decreases and  $Y_2$  gradually increases. When  $X_3$  and  $X_2$  gradually increased within the experiment range,  $Y_1$  gradually increases and  $Y_2$  gradually increases. This was because when  $X_1$  was certain (the input power is certain) the same  $X_2$  was the same material in the unit time force effect is equal,  $X_2$  and  $X_3$  increased to improve the gravity effect of the material, further increasing the mixing movement time of the material in the housing, improve the mixing effect. But at the same time, increased the time of the material attached to the housing and mixing parts. The adhesion strength was improved and the discharge quantity is reduced.

#### **Parameter optimization and verification test**

Set the target parameter the mixing uniformity and the material residual rate to maximize, and the factors parameter to the range of experiment to obtain the optimal working parameter combination of the spiral-ribbon inclined combined mixing device: the speed of main shaft was 48.73 r/min, the full coefficient was 58.45%, and the inclination angle was  $19.10^\circ$ , the overall operation effect being the best. The predicted mixing uniformity will be 88.97% and the material residue rate will be 5.11%.

In order to further verify the reliability and applicability of the mathematical model, the optimization results were tested and verified under the same experiment conditions, while the actual test results and the model prediction values were analysed for error. Considering the operability of the test, the optimization results were adjusted as follows: the spindle speed was 50 r/min, the fullness coefficient was 60%, and the inclination angle was  $19^\circ$ , and three repeated tests were carried out to obtain the best working parameter combination. The average values of the test values of uniformity and material residue

rate were 90.37% and 5.31%, respectively, which were close to the predicted values of the model. The relative error between the actual and predicted values didn't exceed 0.5%, indicating the established model and analysis results were valid.

## CONCLUSIONS

In this paper, mixing uniformity and material residue rate are used as the performance indexes of the diagonal mixing conveyor of straw and manure. Combine with the theoretical analysis of the stress theory to materials in different structures and the test results of prototypes under theoretical assumptions, the following conclusions are drawn:

1) The inclined mixing conveyor completes the feeding, mixing, and conveying of straw silk and cow manure in succession through the spiral-ribbon combined mechanism, which can realize the mixed conveying of straw manure.

2) The result shows that the order of influence of each factor on mixing uniformity is as follows: inclination angle, full coefficient, and speed of main shaft. The order of influence of interaction of factors on mixing uniformity is as follows: speed of main shaft and full coefficient, speed of main shaft and inclination angle, full coefficient and inclination angle. The order of influence of each factor on material residual rate is as follows: full coefficient, speed of main shaft, and inclination angle. The order of influence of interaction of factors on material residual rate is as follows: the speed of main shaft and the full coefficient, full coefficient and inclination angle.

3) According to the response surface method, the optimal parameter combination is as follows: speed of main shaft 50 r/min, full coefficient 60%, inclination angle 19°, corresponding to the mean value of mixing uniformity and material residue rate are 90.37% and 5.31% respectively.

## ACKNOWLEDGEMENT

The study was supported by the Liaoning Province Natural Science Foundation of Innovation Capacity Promotion Joint Fund (2022-NLTS-19-05). The authors thank relevant scholars for their assistance in the literature.

## REFERENCES

- [1] Chen Shan, Han Hui, Zhang Xin, et al. (2020), Analysis on the agricultural ecological cycle model of planting and farming combination (种养结合的农业生态循环模式探析), *Territory & Natural Resources Study*, vol.185, no.2, pp.63-65, Harbin/China.
- [2] Chupshev A., Teryushkov V., Konovalov V., et al. (2019), Functional model of energy consumption for mixing with a vertical paddle mixer [C]. *XII International Scientific Conference on Agricultural Machinery Industry, IOP Conference Series: Earth and Environmental Science*, vol.403, 012102.
- [3] Dong Hongmin, Zuo Lingling, Wei Sha, et al. (2019), Establish manure nutrient management plan to promote green development of integrated crop-livestock production system, *Bulletin of Chinese Academy of Sciences*, vol.34, no.2, pp.180-189, Beijing/China.
- [4] Feng Junxiao, Lin Jia, Li Shizhong, et al. (2017), Calibration of discrete element parameters of particle in rotary solid state fermenters (秸秆固态发酵回转筒内颗粒混合状态离散元参数标定), *Transactions of the CSAM*, vol.46, no.3, pp.208-213, Beijing/China.
- [5] Hewko B.M., Popovich P.V., Diachun A.Y., et al. (2015), The study of bulk material kinematics in a screw conveyor-mixer, *INMATEH - Agricultural Engineering*, vol.47, no.3, pp.155-162, Bucharest / Romania.
- [6] Li Liqiao, Wang Defu, Li Chao, et al. (2017), Design and experimental optimization of combined-type ration mixer of drum and blade (转筒与桨叶组合式日粮混合机设计与试验优化), *Transactions of the CSAM*, vol.48, no.10, pp.67-75, Beijing/China.
- [7] Li Ruxin, Geng Aijun, Zhao He, et al. (2012), Rheologic behavior of chopped corn stalks during rotary compression (碎玉米秸秆卷压过程的流变行为试验), *Transactions of the CSAE*, vol.28, no.18, pp.30-35, Beijing/China.
- [8] Mohammadreza E., Amirsalar Y., Behrooz J., et al. (2020), Assessment of bi-disperse solid particles mixing in a horizontal paddle mixer through experiments and DEM, *Powder Technology*, vol.381, pp.129-140, Lausanne/Switzerland.
- [9] Sakai M., Shigeto Y., Basinskas G., et al. (2015), Discrete element simulation for the evaluation of solid mixing in an industrial blender, *Chemical Engineering Journal*, vol.279, pp.821-839, Lausanne/Switzerland.

- [10] Savinyh P., Aleshkin A., Turbanov N., et al. (2020), Investigation of impact of technological and structural parameters upon energy indicators of work of mixer, *19th International Scientific Conference Engineering for Rural Development, Engineering for Rural Development*, vol.19, pp.1338-1348.
- [11] Simons T.A.H., Bensmann S., Zigan S., et al. (2016), Characterization of granular mixing in a helical ribbon blade blender, *Powder Technology*, vol.293, pp.15-25, Lausanne / Switzerland.
- [12] Ștefan V., Cârdei P., Vlăduț N.V., et al. (2018), Mathematical model for particle motion applied on a manure spreading apparatus used in environmentally friendly technology, *Environmental Engineering and Management Journal*, January, vol.17, no.1, pp. 217-227, Iasi / Romania.
- [13] Ștefan V., David L., Popa L., et al. (2017), Use of theoretical mathematical relations for calculating the application and mass flow rate of a rear delivery vertical axis manure spreader, *16th International scientific conference engineering for rural development proceedings*, vol.16, May 24-26, pp.1284-1291
- [14] Ștefan V., Sfârșu R. & Popa L. (2019), Experimental results on the solid organic fertilizer machine MG 5. *E3S Web of Conferences* 112, 03007.
- [15] Ștefan V., Zaica A., Adrian Iosif. (2021), Research on the uniformity degree of solid organic fertilizers distribution, *INMATEH-Agricultural Engineering*, vol.65, no.3, pp.495-504, Bucharest/Romania. <https://doi.org/10.35633/inmateh-65-51>
- [16] Wang Defu, Dang Chunxue, Huang Huinan, et al. (2020), Mechanism Analysis and parameter optimization of paddle-type ration mixer (桨叶式日粮混合机机理分析与参数优化), *Transactions of the CSAM*, vol.51, no.6, pp.122-131, Beijing/China.
- [17] Wang Defu, Li Chao, Li Liqiao, et al. (2017), Mechanism analysis and parameter optimization of blade-type feed mixer (叶板式饲料混合机混合机理分析与参数优化), *Transactions of the CSAM*, vol.48, no.12, pp.98-104, Beijing/China.
- [18] Wang Ruifang, Li Zhanyong, Dou Rubiao, et al. (2013), Simulation on random motion and mixing characteristic for soybean in rotary drum (水平转筒内大豆颗粒随机运动与混合特性模拟), *Transactions of the CSAM*, vol.44, no.6, pp.93-99, Beijing/China.
- [19] Wang Ruili, Yu Jin, Wang Tiejun, et al. (2021c), Experimental study on molding technology for a mixture of corn straw and cow manure, *BioResources*, vol.16, no.1, pp.1740-1756, USA.
- [20] Wang Tiejun, Wang Ruili, Sun Junde, et al. (2021a), Parameter optimization of the small-scale compost technology with localization maize stover and livestock manure (秸秆-粪便属地化微贮制肥工艺参数优化), *Transactions of the CSAE*, vol.37, no.2, pp.251-257, Beijing/China.
- [21] Wang Tiejun, Wang Tieliang, Cui Hongguang, et al. (2021b), Design and experiment of adjustable feeding straw bale-breaking and rubbing filament machine (喂入调节式秸秆破包揉丝机设计与试验), *Transactions of the CSAM*, vol.52, no.6, pp.148-158, Beijing/China.
- [22] Wulantuya, Qing Lin, Wang Chunguang. (2019), Design of screw-pneumatic coupling conveying device for crushed corn straw (揉碎玉米秸秆螺旋—气力耦合输送装置设计), *Transactions of the CSAE*, vol.35, no.6, pp.29-38, Beijing/China.
- [23] Wulantuya, Wang Chunguang, Qi Shaohua, et al. (2016), Analysis and test of theoretical model of screw conveyor for rubbing and breaking corn straw (揉碎玉米秸秆螺旋输送理论模型分析与试验), *Transactions of the CSAE*, vol.32, no.22, pp.18-26, Beijing/China.
- [24] Xu Xuemeng, Li Feixiang, Li Yongxiang, et al. (2019), Design and experiment of quantitative variable pitch screw (定量变距螺旋结构设计与试验), *Transactions of the CSAM*, vol.50, no.12, pp.89-97, Beijing/China.
- [25] Yu Keqiang, Li Liqiao, He Xun, et al. (2015), Experimental design and principle analysis on paddle-wheel total mixed ration mixer (转轮式全混合日粮混合机试验设计与机理分析), *Transactions of the CSAM*, vol.46, no.7, pp.109-117, Beijing/China.
- [26] Zhang Huipeng. (2020), Big country and small farmers: structural contradiction and governance difficulty - Take the management of agricultural ecological environment as an example, *Journal of China Agricultural University Social Sciences*, vol.37, no.1, pp.15-24, Beijing/China.
- [27] Zhou Jingzhi, Zhou Xingzhi, Feng Junxiao, et al. (2015), Rotary cycle of crushed straw material bed and complete mixing time of layers in rotary cylinder (回转筒内秸秆碎料回转周期和料层完全混合时间研究), *Transactions of the CSAM*, vol.46, no.8, pp.178-185, 238, Beijing/China.